

## Analysis and Characterization of Fe<sub>3</sub>O<sub>4</sub>/Silica Composite from Rice Husk Ash

Susilawati<sup>1\*</sup>, Hariyati Lubis<sup>2</sup>, Timbangan Sembiring<sup>1</sup>, Jeddah Yanti<sup>3</sup>, Syahrani Nabilla Pardede<sup>1</sup>, and Agnes Federova Napitupulu<sup>1</sup>

<sup>1</sup>Department of Physics, Faculty of Mathematics and Natural Sciences, Universitas Sumatera Utara, Medan, 20155, Indonesia

<sup>2</sup>Department of Civil Engineering, Faculty of Engineering, Universitas Amir Hamzah, Medan, 20221, Indonesia

<sup>3</sup>Department of Geography, Faculty of Mathematics and Natural Sciences, Universitas Negeri Makassar, 90222, Indonesia

\*Corresponding Author: [susilawati@usu.ac.id](mailto:susilawati@usu.ac.id)

### ARTICLE INFO

#### Article history:

Received 5 February 2024

Revised 12 February 2024

Accepted 19 February 2024

Available online 29 February 2024

E-ISSN: 2656-0755

P-ISSN: 2656-0747

#### How to cite:

Susilawati, H. Lubis, T. Sembiring, J. Yanti, S. N. Pardede, and A. F. Napitupulu, "Analysis and Characterization of Fe<sub>3</sub>O<sub>4</sub>/Silica Composite from Rice Husk Ash," Journal of Technomaterial Physics, vol. 06, no. 01, pp. 27-32, Feb. 2024, doi: 10.32734/jotp.v6i1.15975.

### ABSTRACT

In this investigation, Fe<sub>3</sub>O<sub>4</sub>/Silica composites were synthesized from rice husk ash utilizing the coprecipitation technique, aiming to elucidate the influence of varied heating temperatures on the surface morphology and elemental composition of the composites. Comprehensive characterizations were conducted employing Fourier Transform Infrared (FTIR) Spectroscopy, X-ray Diffraction (XRD), and Scanning Electron Microscopy (SEM). These analyses unveiled a heterogeneous distribution of Fe<sub>3</sub>O<sub>4</sub> nanoparticles and affirmed the amorphous characteristic of the silica constituent, with the XRD results prominently displaying a broad peak at approximately  $2\theta = 38^\circ$ , signifying the amorphous nature. Despite the alterations in heating temperatures, SEM observations indicated a negligible effect on the nanoparticles' surface morphology, whereas notable variations were discerned in their elemental composition. The outcomes of this study provide insightful contributions to the understanding of the structural properties of Fe<sub>3</sub>O<sub>4</sub>/Silica composites, suggesting avenues for refining synthesis methodologies for enhanced environmental and technological utilization.

**Keywords:** Adsorber, Fe<sub>3</sub>O<sub>4</sub>/Silica, Rice Husk

### ABSTRAK

Pada penelitian ini, komposit Fe<sub>3</sub>O<sub>4</sub>/Silika disintesis dari abu sekam padi dengan menggunakan teknik kopresipitasi, yang bertujuan untuk mengetahui pengaruh suhu pemanasan yang bervariasi terhadap morfologi permukaan dan komposisi unsur komposit. Karakterisasi komprehensif dilakukan dengan menggunakan Spektroskopi Fourier Transform Infrared (FTIR), Difraksi Sinar-X (XRD), dan Scanning Electron Microscopy (SEM). Analisis ini mengungkap distribusi nanopartikel Fe<sub>3</sub>O<sub>4</sub> yang heterogen dan menegaskan karakteristik amorf dari konstituen silika, dengan hasil XRD yang secara mencolok menampilkan puncak yang luas pada sekitar  $2\theta = 38^\circ$ , yang menandakan sifat amorf. Terlepas dari perubahan suhu pemanasan, pengamatan SEM menunjukkan efek yang dapat diabaikan pada morfologi permukaan nanopartikel, sedangkan variasi penting terlihat pada komposisi unsurnya. Hasil dari penelitian ini memberikan kontribusi yang mendalam terhadap pemahaman tentang sifat struktural komposit Fe<sub>3</sub>O<sub>4</sub>/Silika, menunjukkan jalan untuk menyempurnakan metodologi sintesis untuk meningkatkan pemanfaatan lingkungan dan teknologi.

**Kata kunci:** Adsorber, Fe<sub>3</sub>O<sub>4</sub>/Silika, Sekam Padi



This work is licensed under a Creative Commons Attribution-ShareAlike 4.0 International.  
<http://doi.org/10.32734/jotp.v6i1.15975>

## 1. Introduction

The current state of affairs in every aspect of life, such as the rapid increase in population and the growth of industries, has impacted the depletion of clean water supplies [1]. The rising level of pollution due to wastewater containing organic and inorganic compounds from human and industrial activities has garnered significant concern over the last decade [2]. Numerous strategies, including the use of membranes, ion exchange, extraction, and precipitation, have been employed to overcome this problem [3]–[5]. However, adsorption remains a particularly promising method due to its ease of operation and high effectiveness [6], [7]. Industrial wastewater discharged into water bodies often contains organic pathogens and inorganic contaminants, which are extremely harmful to the environment [8].

Several metal oxide adsorbents can be applied to treat wastewater, including magnetite ( $\text{Fe}_3\text{O}_4$ ), titanium dioxide ( $\text{TiO}_2$ ), zinc oxide ( $\text{ZnO}$ ), alumina oxide ( $\text{Al}_2\text{O}_3$ ), magnesium oxide ( $\text{MgO}$ ), and zirconium oxide ( $\text{ZrO}_2$ ). Among these, magnetite nanoparticles ( $\text{Fe}_3\text{O}_4$ ) are particularly intriguing due to their magnetic properties, high surface area, optical and catalytic properties, and strong adsorption bonds to organic pollutants [9]. One of the most promising coating materials for  $\text{Fe}_3\text{O}_4$  is silica ( $\text{SiO}_2$ ). Silica protects  $\text{Fe}_3\text{O}_4$  nanoparticles from oxidation and agglomeration across different pH ranges and enhances their chemical stability and adsorption of hard metal ions. These functions make it suitable for magnetic separators in microbiology and detoxifying biological fluids. Additionally, silica's good hydrophilicity, stability, and biocompatibility enhance the performance of  $\text{Fe}_3\text{O}_4$  nanoparticles in attaching organic molecules to the surface of nanoparticles through covalent bonds. Alizadeh et al. (2020) synthesized  $\text{Fe}_3\text{O}_4/\text{SiO}_2$  for use as an adsorbent in the removal of methylene blue dye [10].  $\text{SiO}_2$  based on natural materials is particularly attractive for study due to the abundance of these materials. For instance, rice husk, a plentiful waste product in Indonesia, contains about 87% - 97% silica by dry weight after complete combustion [11].

Indonesia is often referred to as an agricultural country because a significant portion of its population is employed in the agriculture sector. In this sector, rice stands out as one of the primary products. According to data from the Central Statistics Agency (BPS), Indonesia is projected to produce 55.67 million tons of dry-milled grain (GKG) rice in 2022. Nevertheless, the by-products of rice processing, especially rice husks, have not been utilized optimally. To maximize the use of rice husks, purification technology is required to obtain high-purity silica material. One technique employed to obtain high-purity  $\text{SiO}_2$  is coprecipitation. This chemical fabrication technique causes a solute to precipitate, forming the desired product. Compared to other conventional methods, this technique offers several advantages, including the production of high-purity products, a simple deposition process, and a relatively quick processing time. This makes it possible to produce powders with controlled crystal sizes using this method [12].

This study aimed to synthesize a  $\text{Fe}_3\text{O}_4/\text{SiO}_2$  composite, where  $\text{SiO}_2$  was produced from rice husk ash waste. The synthesis process employed the coprecipitation technique with varied heating temperatures, and the changes in surface morphology were then observed using an SEM-EDX instrument.

## 2. Methods

### 2.1. Synthesis of $\text{SiO}_2$ from Rice Husk

To synthesize  $\text{SiO}_2$ , 500 grams of rice husks were first washed and soaked in distilled water for 24 hours. They were then dried in an oven. Subsequently, the dried rice husks were heated to  $700^\circ\text{C}$  in a furnace to produce ash. The resulting rice husk ash was then crushed. For activation, 50 mL of distilled water and  $\text{ZnCl}$  were added to the ash. The mixture was placed in a closed container and dried in the oven.

### 2.2. Synthesis of $\text{Fe}_3\text{O}_4/\text{SiO}_2$

The synthesis of  $\text{Fe}_3\text{O}_4/\text{SiO}_2$  began with mixing  $\text{SiO}_2$  and  $\text{Fe}_3\text{O}_4$  in ethanol. This was done by stirring the mixture at 500 rpm using a magnetic stirrer. Each mixture was then treated with concentrated  $\text{NH}_4\text{OH}$  and stirred in a fume cupboard using a magnetic stirrer. Subsequently, the solution was removed from the fume cupboard and washed with distilled water. The precipitate was washed with ethanol at 500 rpm until the pH reached 7. Afterward, the precipitate was dried in an oven. The dried samples were crushed for 1 hour to form a powder. Finally, the powder sample underwent characterization using XRD, SEM-EDS, and FTIR.

## 3. Result and Discussion

### 3.1. SEM- EDX Analysis of $\text{Fe}_3\text{O}_4/\text{SiO}_2$ Composites

The SEM images reveal that the distribution of  $\text{Fe}_3\text{O}_4$  nanoparticles is uneven, with many clusters exhibiting the morphology of the  $\text{Fe}_3\text{O}_4$  particles. Figure 3 displays the SEM-EDX results of the  $\text{Fe}_3\text{O}_4/\text{SiO}_2$  composites derived from rice husk ash at various heating temperatures. At  $700^\circ\text{C}$ , the sample's homogeneous surface shows elemental compositions of O = 48.3%, C = 22.4%, Fe = 22.1%, and Si = 7.2%. This suggests

the possibility of interparticle agglomeration among  $\text{Fe}_3\text{O}_4$  nanoparticles to incomplete sample preparation or non-uniform grinding in the furnace [13], [14]. The particles are round, with an 82.84 – 110.9 nm size range. However, the surface morphology images reveal gaps and distances between particles. Overall, while the heating temperatures did not significantly impact the surface morphology of the composites, they did affect the elemental compositions and their respective percentages.

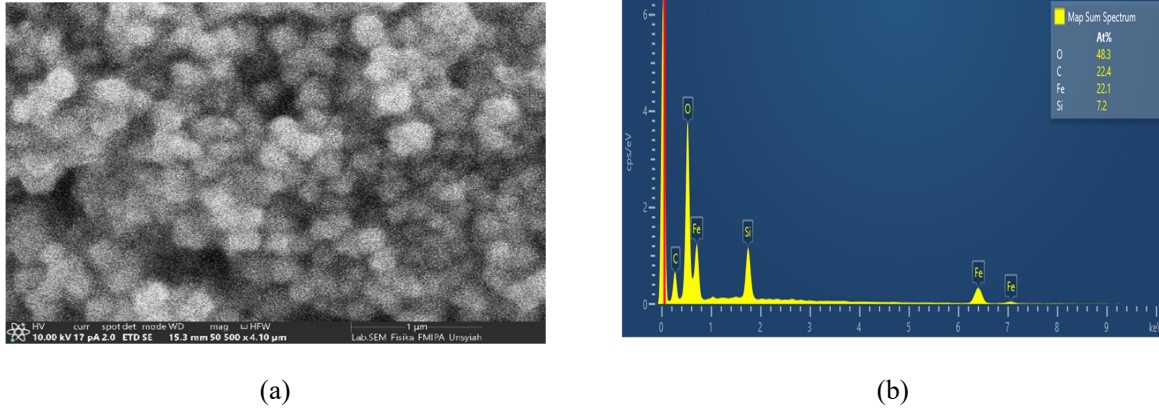


Figure 1. Morphology images and chemical compositions of  $\text{Fe}_3\text{O}_4/\text{SiO}_2$  from rice husk ash at (a)  $T = 700^\circ\text{C}$  with 50000x magnification.

### 3.2. XRD Analysis of $\text{Fe}_3\text{O}_4/\text{SiO}_2$ Composites

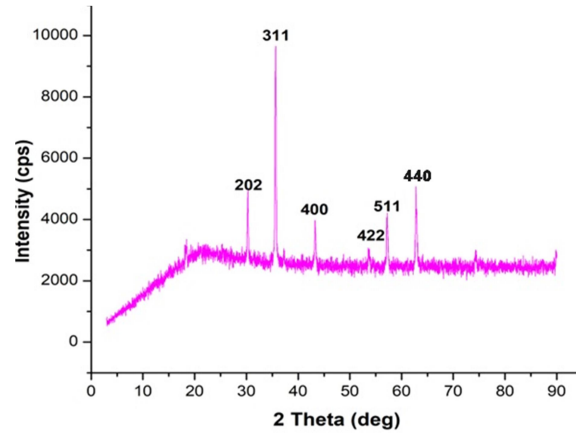


Figure 2. Image of  $\text{Fe}_3\text{O}_4/\text{SiO}_2$  structure from rice husk ash at  $T = 700^\circ\text{C}$ .

Table 1. Peak graphic of XRD in sample.

No.	2-theta (deg)	hkl	Height (cps)	FWHM (deg)	Int. I (cps deg)	Int. W (deg)	Asym. factor
1	30.275(17)	202	1632(117)	0.190(16)	415(18)	0.25(3)	2.2(10)
2	35.608(7)	311	5399(212)	0.186(7)	1433(20)	0.265(14)	1.1(2)
3	43.279(14)	400	1225(101)	0.15(2)	296(14)	0.24(3)	1.8(9)
4	53.589(9)	422	602(71)	0.14(3)	148(15)	0.25(5)	0.5(4)
5	57.149(17)	511	1393(108)	0.22(2)	404(20)	0.29(4)	0.51(19)
6	62.774(11)	440	2052(131)	0.211(15)	591(20)	0.29(3)	1.0(2)

The XRD results of the  $\text{Fe}_3\text{O}_4/\text{SiO}_2$  composite from rice husk material, heated at  $700^\circ\text{C}$ , indicate that the silica ash obtained from well-burned rice husks is either in the initial treatment stage or amorphous. As illustrated in Figure 2, the XRD pattern shows peaks at  $2\theta = 30.275^\circ$ ,  $35.608^\circ$ ,  $43.279^\circ$ ,  $53.589^\circ$ ,  $57.149^\circ$ , and  $62.774^\circ$ , which correspond to the (202), (311), (400), (422), (511), and (440) reflections, respectively. This is evidenced by the sloping peak at around  $2\theta = 38^\circ$ , characteristic of amorphous silica. The XRD

testing determined the crystal structure, the highest peak, and the phase formation of the  $\text{Fe}_3\text{O}_4/\text{SiO}_2$  sample. The XRD patterns of  $\text{Fe}_3\text{O}_4$ ,  $\text{Fe}_3\text{O}_4\text{-SiO}_2$ , and  $\text{Fe}_3\text{O}_4\text{-SiO}_2\text{-NH}_2$  indicate that the crystalline structure of the modified nanoparticles remained unchanged during the process. This suggests that the physical properties of the magnetite particles were not affected by the conjugation and surface modification of the  $\text{Fe}_3\text{O}_4$  nanoparticles. Shao et al. (2012) observed that the  $\text{SiO}_2$  peak is located at a  $2\theta$  angle of  $24^\circ$ , indicating the presence of amorphous silica. The diffraction peak of  $\text{Fe}_3\text{O}_4$  particles increases with the addition of  $\text{SiO}_2$  [15]. According to JCPDS No. 190629, the Bragg peaks are indexed as magnetite. The Miller Indices (hkl) are (220), (311), (400), (422), (511), and (440), corresponding to the  $\text{SiO}_2\text{-Fe}_3\text{O}_4$  peaks. The average crystal size, calculated using the Scherrer equation, is approximately 60 nm [16].

### 3.3. FTIR Analysis of $\text{Fe}_3\text{O}_4/\text{SiO}_2$ Composites

Figure 3 presents the FTIR results of the  $\text{Fe}_3\text{O}_4/\text{SiO}_2$  composite synthesized from rice husk material, heated at  $700^\circ\text{C}$ . The FTIR spectra (Figure 3) also reveal the amorphous nature of the resulting silica ash. The characteristic fingerprint of amorphous silica is evident in three wave number intervals:  $500\text{-}750\text{ cm}^{-1}$ ,  $1200\text{-}1250\text{ cm}^{-1}$ , and  $3300\text{-}3500\text{ cm}^{-1}$ . These wave numbers correspond to the stretching vibrations of asymmetric and symmetric Si-O-Si bonds.

The FTIR test results were conducted to identify the functional groups present in the tested samples. FTIR spectroscopy is a powerful technique that identifies specific functional groups in a material based on their absorption patterns in the infrared region. The wave absorption patterns observed in the FTIR results provide information about the types of chemical bonds and functional groups present in the  $\text{Fe}_3\text{O}_4/\text{SiO}_2$  composite.

The specific peaks in the absorption spectrum correspond to vibrations associated with different chemical bonds. The Fourier Transform Infrared (FTIR) spectrometry spectra of the  $\text{Fe}_3\text{O}_4/\text{SiO}_2$  SNPs revealed certain absorption peaks that suggested the presence of Si-O-Si, O-Si-O, Fe-O, and Fe-O-Si bonds [17]. The FTIR analysis of the  $\text{Fe}_3\text{O}_4/\text{SiO}_2$  composite at a heating temperature of  $700^\circ\text{C}$  confirms the amorphous nature of the resulting silica and highlights specific wave numbers associated with Si-O-Si vibrations. This information contributes to a comprehensive understanding of the structural and chemical characteristics of the synthesized composite material. In other words, these vibrations indicate the presence of silicon-oxygen networks in the amorphous silica structure. The FTIR test results for the  $\text{Fe}_3\text{O}_4/\text{SiO}_2$  composite provide insights into the functional groups formed, as evidenced by the wave absorption patterns observed in the tested samples [18], [19].

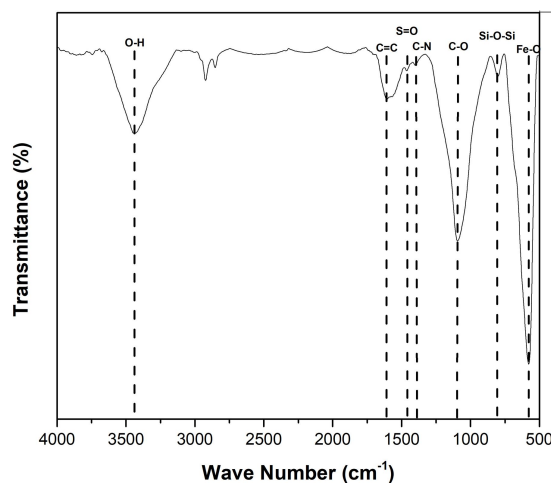


Figure 3. Analysis of  $\text{Fe}_3\text{O}_4/\text{SiO}_2$  clusters from rice husk ash at  $T = 700^\circ\text{C}$ .

## 4. Conclusion

In this comprehensive study, Fourier Transform Infrared (FTIR) Spectroscopy, Scanning Electron Microscopy (SEM), and X-ray Diffraction (XRD) analyses were meticulously employed to explore the impact of varying heating temperatures on the morphological and elemental properties of  $\text{Fe}_3\text{O}_4/\text{Silica}$  composites synthesized from rice husk ash. SEM assessments revealed an uneven distribution of  $\text{Fe}_3\text{O}_4$  nanoparticles and highlighted the minimal influence of thermal treatment on surface morphology. Simultaneously, alterations in elemental composition demonstrated a considerable dependence on the thermal conditions applied, indicating the sensitivity of the composite's chemical properties to heating

temperatures. The FTIR spectroscopy data provided invaluable insights into the chemical bonding and functional groups present in the composites, revealing characteristic absorption bands associated with Si-O-Si and Fe-O vibrations, which further substantiate the formation and integration of  $\text{Fe}_3\text{O}_4$  and silica within the composite structure. The XRD analysis was particularly revealing, identifying the amorphous nature of silica through a broad diffraction peak at approximately  $2\theta = 38^\circ$  and elucidating the crystalline structure of  $\text{Fe}_3\text{O}_4$ , thus offering profound insights into the composite's phase composition and structural integrity. These combined observations from SEM, FTIR, and XRD analyses significantly advance our understanding of the structural and chemical dynamics of  $\text{Fe}_3\text{O}_4$ /Silica composites. This research underscores the critical role of synthesis parameters in defining the composites' morphological, elemental, and bonding characteristics, laying a foundational basis for optimizing these materials for specific applications in environmental and technological fields where precise material properties are paramount for enhanced operational efficiency.

### Acknowledgments

The authors would like to take this opportunity to express their profound gratitude to Universitas Sumatera Utara for facilitating the research experiment, which was instrumental in ensuring the project's successful conclusion.

### References

- [1] N. S. Alkayal and M. A. Hussein, "Photocatalytic Degradation of Atrazine under Visible Light Using Novel  $\text{Ag@Mg}_4\text{Ta}_2\text{O}_9$  Nanocomposites," *Sci. Rep.*, vol. 9, no. 1, pp. 1–11, 2019, doi: 10.1038/s41598-019-43915-y.
- [2] D. Iark *et al.*, "Enzymatic degradation and detoxification of azo dye Congo red by a new laccase from *Oudemansiella canarii*," *Bioresour. Technol.*, vol. 289, no. April, p. 121655, 2019, doi: 10.1016/j.biortech.2019.121655.
- [3] K. C. Rani, A. Naik, R. S. Chaurasiya, and K. S. M. S. Raghavarao, "Removal of toxic Congo red dye from water employing low-cost coconut residual fiber," *Water Sci. Technol.*, vol. 75, no. 9, pp. 2225–2236, 2017, doi: 10.2166/wst.2017.109.
- [4] G. Chen *et al.*, "Signatures of tunable superconductivity in a trilayer graphene moiré superlattice," *Nature*, vol. 572, no. 7768, pp. 215–219, 2019, doi: 10.1038/s41586-019-1393-y.
- [5] C. Azmiyawati, P. I. Pratiwi, and A. Darmawan, "New Silica Magnetite Sorbent: The Influence of Variations of Sodium Silicate Concentrations on Silica Magnetite Character," *IOP Conf. Ser. Mater. Sci. Eng.*, vol. 349, no. 1, 2018, doi: 10.1088/1757-899X/349/1/012012.
- [6] Y. Wei, B. Han, X. Hu, Y. Lin, X. Wang, and X. Deng, "Synthesis of  $\text{Fe}_3\text{O}_4$  nanoparticles and their magnetic properties," *Procedia Eng.*, vol. 27, no. 2011, pp. 632–637, 2012, doi: 10.1016/j.proeng.2011.12.498.
- [7] M. A. I. Permana, N. Nandaliarsyad, A. Q. A. Haq, M. Nawansari, and C. Mulyana, "Kajian Potensi Silica Scaling Pada Pipa Produksi Pembangkit Listrik Tenaga Panas Bumi (Geothermal)," *J. Mater. dan Energi Indones.*, vol. 7, no. 01, p. 39, 2017, doi: 10.24198/jmei.v7i01.12255.
- [8] S. Taib and E. Suharyadi, "Sintesis Nanopartikel Magnetite ( $\text{Fe}_3\text{O}_4$ ) dengan Template silika ( $\text{SiO}_2$ ) dan Karakterisasi Sifat Kemagnetannya," *Indones. J. Appl. Phys.*, vol. 5, no. 01, p. 23, 2015, doi: 10.13057/ijap.v5i01.256.
- [9] S. Yatmani, N. Maulida, and D. Suastiyanti, "Sintesis Material Nanomultiferroic Berbasis Barium Titanate dan Bismuth Ferrite dengan Variasi Temperatur dan Waktu Sintering," *Pros. SNIPS 2018 Sint.*, pp. 102–109, 2018.
- [10] A. Alizadeh, M. Fakhari, Z. Safaei, M. M. Khodeai, E. Repo, and A. Asadi, "Ionic liquid-decorated  $\text{Fe}_3\text{O}_4@ \text{SiO}_2$  nanocomposite coated on talc sheets: An efficient adsorbent for methylene blue in aqueous solution," *Inorg Chem Commun*, vol. 121, p. 108204, Nov. 2020, doi: 10.1016/J.INOCHE.2020.108204.
- [11] E. Evan, P. Pardoyo, and A. Darmawan, "Pembuatan Nanosilika dari Abu Sekam Padi pada Variasi pH Sol Gel," *Greensph. J. Environ. Chem.*, vol. 2, no. 1, pp. 8–13, 2022, doi: 10.14710/gjec.2022.14720.
- [12] M. Abareshi, E. K. Goharshadi, S. Mojtaba Zebarjad, H. Khandan Fadafan, and A. Youssefi, "Fabrication, characterization and measurement of thermal conductivity of  $\text{Fe}_3\text{O}_4$  nanofluids," *J. Magn. Magn. Mater.*, vol. 322, no. 24, pp. 3895–3901, 2010, doi: 10.1016/j.jmmm.2010.08.016.
- [13] A. Karimi, M. Goharkhah, M. Ashjaee, and M. B. Shafii, "Thermal Conductivity of  $\text{Fe}_2\text{O}_3$  and  $\text{Fe}_3\text{O}_4$  Magnetic Nanofluids Under the Influence of Magnetic Field," *Int. J. Thermophys.*, vol. 36, no. 10–11, pp. 2720–2739, 2015, doi: 10.1007/s10765-015-1977-1.

- [14] H. Xie, J. Wang, T. Xi, Y. Liu, and F. Ai, "Dependence of the thermal conductivity on nanoparticle-fluid mixture on the base fluid," *J. Mater. Sci. Lett.*, vol. 21, no. 19, pp. 1469–1471, 2002, doi: 10.1023/A:1020060324472.
- [15] G. N. Shao *et al.*, "Two step synthesis of a mesoporous titania-silica composite from titanium oxychloride and sodium silicate," *Powder Technol.*, vol. 217, pp. 489–496, 2012, doi: 10.1016/j.powtec.2011.11.008.
- [16] M. Pilloni *et al.*, "PEGylation and preliminary biocompatibility evaluation of magnetite-silica nanocomposites obtained by high energy ball milling," *Int. J. Pharm.*, vol. 401, no. 1–2, pp. 103–112, 2010, doi: 10.1016/j.ijpharm.2010.09.010.
- [17] D. X. Luong *et al.*, "Gram-scale bottom-up flash graphene synthesis," *Nature*, vol. 577, no. 7792, pp. 647–651, 2020, doi: 10.1038/s41586-020-1938-0.
- [18] H. Ardiyanti, D. Puspitarum, O. F. Maryana, and W. A. Pujakesuma, "Synthesis and Bonding Analysis of Magnetite ( $\text{Fe}_3\text{O}_4$ )/silica ( $\text{SiO}_2$ ) Composite Based on Sugarcane Bagasse," *J. Sci. Appl. Technol.*, vol. 2, no. 1, pp. 197–200, 2019, doi: 10.35472/281425.
- [19] T. Sembiring, D. Siburian, and M. Rianna, "ZnMnFe<sub>2</sub>O<sub>4</sub> particle synthesized by natural iron sand for making permanent magnetic material," *Mater. Sci. Energy Technol.*, vol. 6, pp. 124–129, 2023, doi: 10.1016/j.mset.2022.12.005.